

# DNA binding and oligomerization of NtrC studied by fluorescence anisotropy and fluorescence correlation spectroscopy

Franz W. Sevenich<sup>†</sup>, Jörg Langowski, Verena Weiss<sup>1</sup> and Karsten Rippe<sup>\*</sup>

Deutsches Krebsforschungszentrum, Abteilung Biophysik der Makromoleküle, Im Neuenheimer Feld 280, D-69120 Heidelberg, Germany and <sup>1</sup>Universität Konstanz, Fakultät für Biologie, Universitätsstraße 10, D-78464 Konstanz, Germany

Received January 15, 1998; Accepted January 27, 1998

## ABSTRACT

**Fluorescence anisotropy and fluorescence correlation spectroscopy measurements of rhodamine-labeled DNA oligonucleotide duplexes have been used to determine equilibrium binding constants for DNA binding of the prokaryotic transcription activator protein NtrC. Measurements were made with wild-type NtrC from *Escherichia coli* and the constitutively active mutant NtrC<sup>S160F</sup> from *Salmonella* using DNA duplexes with one or two binding sites. The following results were obtained: (i) the dissociation constant  $K_d$  for binding of one NtrC dimer to a single binding site was the same for the wild-type and mutant proteins within the error of measurement. (ii) The value of  $K_d$  decreased from  $1.4 \pm 0.7 \times 10^{-11}$  M at 15 mM K acetate to  $5.8 \pm 2.6 \times 10^{-9}$  M at 600 mM K acetate. From the salt dependence of the dissociation constant we calculated that two ion pairs form upon binding of one dimeric protein to the DNA. (iii) Binding of two NtrC dimers to the DNA duplex with two binding sites occurred with essentially no cooperativity. Titration curves of NtrC<sup>S160F</sup> binding to the same duplex demonstrated that more than two protein dimers of the mutant protein could bind to the DNA.**

## INTRODUCTION

NtrC (nitrogen regulatory protein C, also designated nitrogen regulator I or NR<sub>I</sub>) from enteric bacteria is one of the activator proteins of RNA polymerase complexed with the  $\sigma^{54}$  sigma factor (RNAP- $\sigma^{54}$  holoenzyme) for a variety of genes that are involved in nitrogen utilization (1). The distal location of the NtrC binding sites found *in vivo* requires looping of the intervening DNA for interaction with RNAP- $\sigma^{54}$  at the promoter (2–5). The looped complex between NtrC and RNAP- $\sigma^{54}$  that can form in the presence of ATP has been visualized by electron microscopy (6) and scanning force microscopy (7). NtrC is a response regulator that belongs to the protein family of two-component

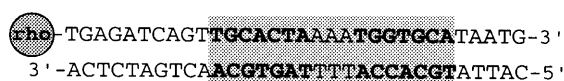
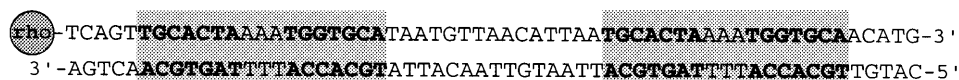
signal transduction systems. It is regulated as a transcriptional activator by phosphorylation at Asp54 of the conserved receiver domain (8,9). *In vivo* the cognate histidine kinase NtrB (nitrogen regulatory protein B, also designated nitrogen regulator II or NR<sub>II</sub>) autophosphorylates under nitrogen limitation conditions and serves as a phosphate donor for this reaction (8,10). Because of its autophosphatase activity the phosphorylated protein is not stable in solution. The half-life of the phosphorylated protein is ~4 min at 37°C (10,11). Constitutively active mutants of NtrC that do not require phosphorylation to activate transcription by RNAP- $\sigma^{54}$  have been described (12–14). In particular, a substitution of serine to phenylalanine in the central domain close to the ATP binding motif results in the mutant NtrC<sup>S160F</sup>, which shows some transcriptional activity without being phosphorylated.

NtrC is a dimer in solution (15,16) and binds as a dimer to a single binding site, as demonstrated by gel electrophoretic analysis (17) and analytical ultracentrifugation (16). Phosphorylated wild-type NtrC and the NtrC<sup>S160F</sup> mutant bind with high cooperativity to two adjacent binding sites, as shown by nitrocellulose filter binding, gel shift experiments and quantitative DNA footprinting (17–19). In a number of studies it has been concluded that oligomerization of phosphorylated NtrC dimers is required for formation of an active NtrC complex (17,20,21). Higher order complexes of NtrC dimers have been observed by electron microscopy (6,17,22) and scanning force microscopy (7,21). The complexes were too unstable to be studied by gel electrophoresis (17). However, a detailed analysis of the different association states of wild-type NtrC protein has been conducted recently by analytical ultracentrifugation (16).

Here we have used thermodynamically rigorous fluorescence spectroscopy measurements to follow binding of NtrC to DNA. Equilibrium binding of NtrC to DNA was monitored by fluorescence anisotropy (FA) and fluorescence correlation spectroscopy (FCS) measurements. The experiments were conducted with DNA oligonucleotide duplexes which carried either one (ES-1<sub>rho</sub>) or two (ES-2<sub>rho</sub>) NtrC binding sites and which were labeled with the fluorescent dye tetramethylrhodamine (Fig. 1). These duplexes showed a certain (low) fluorescence anisotropy in the absence of bound protein. The anisotropy

<sup>\*</sup>To whom correspondence should be addressed. Tel: +49 6221 423392; Fax: +49 6221 423391; Email: karsten.rippe@dkfz-heidelberg.de

Present address: <sup>†</sup>Philipps-Universität Marburg, Institut für pharmazeutische Chemie, Marbacher Weg 6, D-35032 Marburg, Germany

ES-1<sub>rho</sub> DNA duplex (single NtrC binding site)ES-2<sub>rho</sub> DNA duplex (two NtrC binding sites)

**Figure 1.** DNA oligonucleotide duplexes ES-1<sub>rho</sub> (32 bp) and ES-2<sub>rho</sub> (59 bp) used for the binding studies. The nucleotides responsible for the dyad symmetry of the binding sites are shaded grey. The NtrC binding site in these duplexes corresponds to the high affinity NtrC binding site overlapping the promoter of *ntrB* (18).

increased if protein was bound to the duplex. This is due to reduced rotational mobility of the protein–DNA complex. According to the Perrin equation (23) anisotropy of a fluorescent complex increases with its volume. Thus changes in anisotropy of fluorescently labeled DNA duplexes can be exploited to monitor protein binding and also protein–protein interactions if they involve a protein–DNA complex. This approach has been used successfully in a number of studies (24–27).

FCS measures mean diffusion times and concentrations by evaluating fluctuations in the fluorescence intensity that have their origin in the Brownian motion of fluorophores through a small volume element. This volume element is defined by the focus of the excitation light beam, with dimensions of  $\sim 0.3 \times 0.3 \times 1.6 \mu\text{m}$  ( $\sim 2 \times 10^{-16}$  l) for the instrument used here. The measured fluctuations in the fluorescence signal depend on the speed at which the fluorophore moves through the focus. Since the diffusion time of rhodamine-labeled DNA duplexes increased upon binding of protein, determination of the diffusion time via FCS can be used to follow the binding process. The principles of FCS were developed more than 20 years ago (28–30). However, only technical improvements made over the last few years have led to an increasing number of applications for this technique (31–37). Both FA and FCS measurements are non-invasive and salt concentration, pH and temperature can be controlled over a wide range. Protein–DNA interactions can be quantified free in solution to derive binding parameters from the analysis of titration curves, as done here for DNA binding of NtrC.

## MATERIALS AND METHODS

### DNA oligonucleotide duplexes

HPLC-purified DNA oligonucleotides were purchased from MWG Biotech (Ebersberg, Germany). One of the strands in the duplexes studied was labeled with tetramethylrhodamine attached to the 5'-end of one oligonucleotide via a C<sub>6</sub> aminoalkyl linker. DNA fragment ES-1<sub>rho</sub> contained a single symmetrical binding site, while fragment ES-2<sub>rho</sub> had two identical binding sites whose centers are separated by exactly three turns of DNA (Fig. 1). The extinction coefficients of the single strands were determined as described (38) from the extinction coefficients of the dinucleotide composition according to the data set presented in Puglisi and Tinoco (39). The calculated values for the single strands were corrected for formation of secondary structure by recording

melting curves of the single strands and extrapolation of the linear increase in extinction coefficient between 50–80°C and 25°C. By this procedure we determined  $\epsilon_{260}$  values at 25°C of 341 000 (rhodamine-labeled strand in ES-1<sub>rho</sub>), 303 000 (complementary strand in ES-1<sub>rho</sub>), 598 000 (rhodamine-labeled strand in ES-2<sub>rho</sub>) and 531 000 M<sup>-1</sup>cm<sup>-1</sup> (complementary strand in ES-2<sub>rho</sub>) for the DNA oligonucleotides shown in Figure 1. The contribution of rhodamine to the absorbance at 260 nm was determined from the spectrum of tetramethylrhodamine 5-isothiocyanate to be 36% of the rhodamine absorbance at 554 nm. Since at the latter wavelength no DNA absorbance is observed the rhodamine absorbance at 260 nm could be extracted from the absorbance spectra of the rhodamine-labeled DNA oligonucleotides.

Duplexes were prepared by mixing 10  $\mu\text{M}$  complementary single strands in 10 mM Tris–HCl, pH 7.5, 0.1 mM EDTA and annealing by heating to 70°C followed by slow cooling to room temperature over several hours. With the known concentrations of the single-stranded stocks the extinction coefficients of the duplexes were determined from absorbance measurements to be  $\epsilon_{260} = 478\,000$  (ES-1<sub>rho</sub>) and  $904\,000\text{ M}^{-1}\text{cm}^{-1}$  (ES-2<sub>rho</sub>) at 25°C in 10 mM Tris–HCl, pH 7.5, 10 mM NaCl and 0.1 mM EDTA. Analysis of the duplexes on native polyacrylamide gels and titration of single strands with the respective complementary strand were conducted as described (40) to check the purity of the sample and the stoichiometry of duplex formation. Gel electrophoretic analysis of the samples of ES-1<sub>rho</sub> and ES-2<sub>rho</sub> DNA used for the fluorescence measurements showed that >95% of the DNA was in the duplex conformation.

### Plasmids and proteins

Wild-type NtrC was purified as described (20). For overexpression of NtrC<sup>S160F</sup> the protein expression vector pNTRC-1 was constructed by cutting plasmid pJES312 (41) with *Nde*I and *Bam*HI and ligating the resulting fragment, carrying the gene encoding NtrC<sup>S160F</sup> from *Salmonella*, into the same sites in pET15b (Novagen). The sequence of the *NtrC*<sup>S160F</sup> gene in pNTRC-1 was confirmed by DNA sequencing. From this vector NtrC<sup>S160F</sup> was expressed with an additional N-terminal His tag having the sequence MGSSHHHHHHSSGLVPRGS, which allows affinity purification using a Ni-chelating resin. Expression and purification of NtrC<sup>S160F</sup> from pNTRC-1 was according to the same procedure used to purify the His-tagged mutant protein NtrC<sup>D54E,S160F</sup> (7). The purified protein stocks were kept at

–20°C in a buffer containing 10 mM Tris–HCl, pH 8.0, 50 mM KCl, 0.1 mM EDTA, 1 mM DTT and 50% glycerol (v/v). The extinction coefficients of NtrC were calculated from the amino acid sequence to be 46 400 (monomer) and 92 800 M<sup>-1</sup>cm<sup>-1</sup> (dimer) at 280 nm (42).

### Fluorescence anisotropy measurements

Fluorescence anisotropy measurements were done with a SLM 8100 fluorescence spectrometer (SLM Aminco Inc.) and either a L- or T-format set-up. The excitation wavelength and the left emission channel wavelength were selected with double-grated monochromators using a 16 nm bandpass for maximum intensity. In the right emission channel scattered light was suppressed with a 570 nm longpass filter. Excitation was at 540 nm and the emission monochromator of the left emission channel was set to 580 nm. For each anisotropy value five measurements were taken and averaged. The integration time was 8 s for the L- and 4 s for the T-format measurements. Using this integration time both measuring methods showed about the same standard deviation.

For titration, cuvettes (10 × 4 mm) were silylated with a 5% solution of trimethylsilylchloride in toluene. The binding buffer, which was also used in the FCS experiments, contained 10 mM Tris–acetate, pH 8.0, 0.1 mM EDTA, 0.1 mg/ml BSA, 1 mM DTT and 0.1% NP-40 detergent (Boehringer Mannheim, Germany) and was supplemented with 15, 150 or 600 mM potassium acetate as indicated. All measurements were made at 25°C. To 500 µl DNA solution in the given buffer was added stepwise a protein solution diluted in the same buffer. During the experiment the protein stock solution was kept on ice. Depending on the protein concentration, up to 200 µl protein solution was added in total. The decrease in DNA concentration during the titration was taken into account in the analysis of the data.

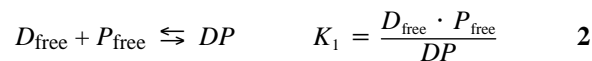
### Data analysis of fluorescence anisotropy measurements

A single step binding model was used for the analysis of the binding isotherm of DNA fragment ES-1<sub>rho</sub> (one NtrC binding site). The binding isotherm for this equilibrium can be solved analytically (24). The data were fitted to the analytical formula (equation 1) using the Marquardt non-linear least squares algorithm. Parameters of the fit were the anisotropies of free and bound DNA ( $A_D$  and  $A_{DP}$ ) and the dissociation constant  $K_d$ .

$$A = A_D + (A_{DP} - A_D) \frac{\alpha - \sqrt{\alpha^2 - 4 \cdot D_{\text{tot}} \cdot P_{\text{tot}}}}{2 \cdot D_{\text{tot}}} \quad \text{with } \alpha = D_{\text{tot}} + P_{\text{tot}} + K_{\text{dis}} \quad \mathbf{1}$$

The parameter  $\theta$  equals the degree of binding. The total concentration of DNA duplex  $D_{\text{tot}}$  and protein  $P_{\text{tot}}$  (corresponding to the concentration of NtrC dimers) was known in these experiments. Equation 1 implicitly assumes that anisotropy is a linear function of the concentrations of the fluorescent species. This assumption is correct only if the quantum yield and the absorption coefficients do not change upon binding. To confirm that this was the case for the system studied here the fluorescence emission spectra of free ES-1<sub>rho</sub> and ES-2<sub>rho</sub> DNA were compared with the emission spectrum obtained after addition of saturating NtrC protein concentrations. Since the intensities and shape of the fluorescence emission spectrum showed virtually no change upon binding of protein the simple formula of equation 1 could be used to analyze the measurements.

For binding of NtrC to the ES-2<sub>rho</sub> fragment, which has two binding sites, the model is more complex. Under our reaction conditions no more than two wild-type NtrC dimers bound to the ES-2<sub>rho</sub> fragment. Thus a two-step model where one and subsequently a second protein dimer is bound to the DNA accounts for this situation. This model is described by the macroscopic dissociation constants  $K_1$  for binding of one protein dimer and  $K_2$  for binding of the second protein dimer.



In these and in the following equation  $P$  designates an NtrC dimer. Taking into account that the two binding sites are identical, the dissociation constants can be expressed in terms of the microscopic dissociation constant for a single site  $k_d$ , which equals the macroscopic dissociation constant  $K_d$  determined from binding to duplex ES-1<sub>rho</sub> and a cooperativity constant  $k_{12}$  as defined in Ackers *et al.* (43), which gives equation 4.

$$K_1 = \frac{k_d}{2} \quad \text{and} \quad k_{12} = \frac{4 \cdot K_1}{K_2} \quad \mathbf{4}$$

A value of  $k_{12} = 1$  would indicate that binding to the two sites is independent, whereas values of  $k_{12} > 1$  would represent positive cooperativity and  $k_{12} < 1$  negative cooperativity. For analysis of the titration curves of ES-2<sub>rho</sub> with the NtrC<sup>S160F</sup> mutant a model was used in which in a first step two NtrC<sup>S160F</sup> dimers bind highly cooperatively ( $k_{12} > 40$ ) to the DNA (equations 2 and 3) and in a second step two additional dimers bind, also in a cooperative manner, to this complex, with a dissociation constant  $K_3$ , to form a tetramer of dimers.



The data were fitted to these two models using the program BIOEQS (44,45). BIOEQS fits the  $\Delta G$  of formation of each species in the model to the data, setting the free energies of free protein and free DNA to zero. Thus for binding of wild-type NtrC (see equations 2 and 3) the fitted parameters included the  $\Delta G$  values corresponding to dissociation constants  $K_1$  and  $K_2$  and anisotropies for free DNA duplex and the 1:1 and the 2:1 protein–DNA complexes. For binding of NtrC<sup>S160F</sup> according to the mechanism described by equations 2, 3 and 5 the fitted parameters were  $\Delta G$  of formation, corresponding to  $K_1 \cdot K_2$  (formation of a complex of ES-2<sub>rho</sub> with two NtrC<sup>S160F</sup> dimers) and  $K_3$  (formation of a complex of ES-2<sub>rho</sub> with four NtrC<sup>S160F</sup> dimers) and anisotropies for free DNA and the 2:1 and 4:1 protein–DNA complexes.

### Fluorescence correlation spectroscopy measurements

Measurements were made in a Confocor instrument (Zeiss, Jena and Evotec, Hamburg). An argon laser with 20 mW power at 514 nm was focused by a water immersion Zeiss C Apochromat 40 × 1.2 objective. A 50 µm pinhole was used in the confocal detection channel. The samples were measured on lab-tek chamber slides with eight chambers and an ~140 µm thick cover slide on the bottom (Nunc, Denmark). The focus of the lens was placed inside the solution to be analyzed and ~200 µm above the

inner surface of the cover slide. The intensity of the fluorescence signal was reduced to ~20 kHz (~50  $\mu$ W incident laser power) by attenuating the excitation laser beam with an appropriate neutral density filter to avoid bleaching of the dye molecules. All experiments were carried out with 1 nM ES-1<sub>rho</sub> in the same binding buffer as used for the FA measurements and the indicated potassium acetate concentrations. At the beginning of each experiment the diffusion time of DNA fragment ES-1<sub>rho</sub> was determined by averaging five measurements of 200 s each. As outlined below, this measurement was also used to determine the instrument parameters, which were dependent on the size of the focus volume which varied slightly from one experiment to another. After addition of protein solution and an incubation time of ~4 min to reach equilibrium the correlation functions were recorded for 100 s for each point of the titration.

### Data analysis of fluorescence correlation spectroscopy measurements

The correlation functions for titration of ES-1<sub>rho</sub> DNA with wt-NtrC were fitted with the FCS access fit software package according to the extended correlation function including triplet states (46).

$$G(\tau) = 1 + \frac{1}{N(1 - \bar{T}_{eq})} \cdot \left[ (1 - \theta) \left(1 + \frac{\tau}{\tau_1}\right)^{-1} \left(1 + \frac{\tau}{\tau_1 \cdot k_{SP}^2}\right)^{-1/2} + \theta \left(1 + \frac{\tau}{\tau_2}\right)^{-1} \left(1 + \frac{\tau}{\tau_2 \cdot k_{SP}^2}\right)^{-1/2} \right] \cdot \left[ 1 - \bar{T}_{eq} \left(1 - \exp\left(-\frac{\tau}{\tau_T}\right)\right) \right] \quad 6$$

Equation 6 describes the correlation function for two species, the free DNA with diffusion time  $\tau_1$  and the wt-NtrC–DNA complex with diffusion time  $\tau_2$ . This treatment is only valid if the quantum yield and the extinction coefficient of the fluorophore do not change upon binding, as was the case for the system studied here (see above). The fractional degree of binding is given by  $\theta$ . From measurements of the free DNA ( $\theta = 0$ ) in the absence of protein the diffusion time  $\tau_1$ , the structure parameter  $k_{SP}$ , the triplet time constant  $\tau_T$  and the triplet amplitude  $\bar{T}_{eq}$  were determined for each experiment. At saturating protein concentrations ( $\theta = 1$ ) the diffusion time  $\tau_2$  of the protein–DNA complex could be measured. With the ratio of the diffusion times  $\tau_1$  and  $\tau_2$  of the two species the ratio of their translational diffusion constants  $D_1$  and  $D_2$  is given by equation 7:

$$\frac{\tau_2}{\tau_1} = \frac{D_1}{D_2} \quad 7$$

Accordingly, in experiments where no total saturation of the DNA was reached during titration the diffusion time of the complex  $\tau_2$  could be calculated from the measured diffusion time of the free DNA and the previously determined ratio of the diffusion constants. This was important, since the absolute values of diffusion times are dependent on the focus volume, which could vary between different experiments. The degree of binding  $\theta$  remained the only unknown parameter and was determined from equation 6 at each titration point. The resulting  $\theta$  values were fitted to equation 8, which corresponds to equation 1 used for analysis of the fluorescence anisotropy measurements.

$$\theta = \frac{\alpha - \sqrt{\alpha^2 - 4 \cdot D_{tot} \cdot P_{tot}}}{2 \cdot D_{tot}}$$

## RESULTS

### Stoichiometric binding to a single binding site

To study binding of NtrC to a single binding site we used a synthetic oligonucleotide, ES-1<sub>rho</sub>, carrying site Lp, which in the *in vivo* sequence overlaps the promoter for *ntrB* (Fig. 1). First we determined the concentration of active NtrC dimers in our protein stock solution from the FA monitored titration with DNA duplex ES-1<sub>rho</sub> (Fig. 2A). For wild-type NtrC anisotropy increased linearly with added protein in the initial part of the curve. Thus at the beginning the added protein was bound quantitatively to the DNA. The anisotropy changes became smaller and finally reached a plateau. The plateau reflects anisotropy of the 1:1 complex of the DNA fragment with one NtrC dimer. Extrapolation of the initial linear increase to the final anisotropy yielded the point at which equimolar amounts of protein were added to the solution.

In contrast to wild-type NtrC, mutant NtrC<sup>S160F</sup> showed no plateau in its binding isotherm (Fig. 2A). Two linear sections could be distinguished. The first resulted from the strong binding of one NtrC dimer, the second was assigned to additional binding of NtrC dimers to the DNA–protein complex. The intersection of the extrapolated linear regions led to the equivalence point, i.e. the point where the ES-1<sub>rho</sub> DNA binding site was saturated with protein.

From the equivalence points and the known DNA concentrations we determined the concentration of active NtrC dimer in our protein stock solutions. The measurements of protein activity were repeated several times. They showed a decrease from 95 to 76% activity during storage of the protein stocks at –20°C over several months, as compared with the protein concentration determined from the initial absorbance measurements. The concentrations of active protein calculated from the stoichiometric titrations determined by either FA or FCS agreed well with concentrations determined by gel shift assays (data not shown).

### Dissociation constants for the single binding site

At 600 mM potassium acetate and a DNA concentration of 2.5 nM (Fig. 2B) the weaker binding of additional proteins of NtrC<sup>S160F</sup> could be neglected and the data were fitted accurately by a 1:1 binding model (equation 1). The fit yielded an anisotropy value for the complex identical for both wild-type and mutant NtrC. With the two anisotropy values for the complex and the free DNA fragment ( $A_{DP}$  and  $A_D$  in equation 1) the degree of binding  $\theta$  could be calculated. This value is shown on the ordinate in Figure 2B. For NtrC<sup>S160F</sup> we obtained a  $K_d$  of  $5.2 \pm 0.5$  nM at 600 mM potassium acetate. Corresponding titrations for wild-type NtrC yielded a  $K_d$  of  $4.2 \pm 0.9$  nM. These results show that wild-type NtrC and mutant NtrC<sup>S160F</sup> bind equally strongly to the single DNA binding site.

The binding of wild-type NtrC to ES-1<sub>rho</sub> duplex was also studied by FCS. Typical correlation curves obtained at different protein concentrations are displayed in Figure 3A. According to equation 6 the intersection with the ordinate is proportional to the reciprocal of the number of particles. The observed increase in the intersection point as more complexes are formed is due to dilution of the solution by addition of protein. Formation of triplet states is detected by the initial decrease in the function in the  $\mu$ s range.

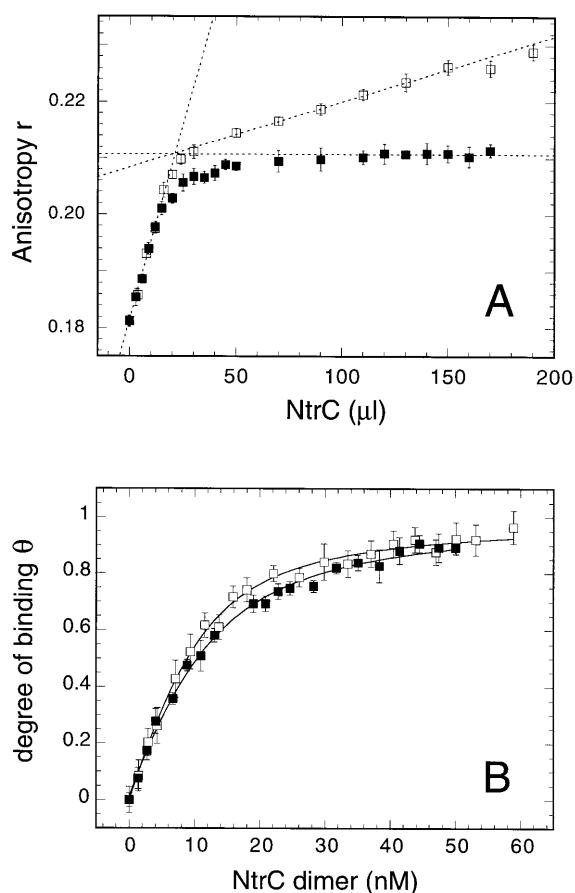


**Figure 2.** Fluorescence anisotropy measurements of NtrC. **(A)** Stoichiometric titrations to determine the concentration of active protein. Anisotropy of a DNA solution is shown as a function of the volume of added protein solution. The DNA solution contained 10 nM tetramethylrhodamine-labeled DNA fragment ES-1<sub>rho</sub> and 150 mM potassium acetate in standard buffer. (—■—) Wild-type NtrC was added to the DNA solution. The dotted lines are the linear regression analysis for 0–15  $\mu\text{l}$  added protein and the mean value for anisotropy from 90 to 170  $\mu\text{l}$ . (—□—) NtrC<sup>S160F</sup> was added to the DNA solution. The dotted lines show the linear regression analysis for 0–12  $\mu\text{l}$  and 60–150  $\mu\text{l}$  added protein. The concentration of active wt-NtrC and NtrC<sup>S160F</sup> was approximately the same in the solutions added, since the initial linear increase in fluorescence anisotropy was almost identical for both proteins. **(B)** Binding isotherms of NtrC. Data are shown for wild-type NtrC (—■—) and NtrC<sup>S160F</sup> (—□—). The solid lines represent the fitted curve determined according to equation 1. The degree of binding was calculated from the anisotropy values for free and bound DNA that were parameters of the fit. The solutions contained 2.5 nM ES-1<sub>rho</sub> and 600 mM potassium acetate.

At the excitation intensities used we measured no more than 10% triplet contribution. The characteristic diffusion times are shown by the decrease in the 0.5 ms segment of the correlation function. As the difference in the two diffusion times of free and bound DNA is fairly small, it is not possible to extract the diffusion coefficients from a free two component fit to the correlation function. Therefore, the diffusion times of free and protein-bound DNA were determined from the correlation functions with no protein and excess of protein in the solution from the fit to a one component model (equation 6,  $\theta = 0$  or  $\theta = 1$ ). As described in Materials and Methods, titration curves can be obtained from the FCS curves by fitting a two species model with

predetermined diffusion times to the correlation functions. Two representative titrations, one at 15 and one at 600 mM K acetate are depicted in Figure 3B. A fit of multiple data sets to equation 8 yielded average values of  $0.014 \pm 0.010$  nM (15 mM K acetate) and  $7.3 \pm 2.5$  nM (600 mM K acetate) for the dissociation constant. The FCS titration at 600 mM salt presented in Figure 3B did not lead to complete saturation of the DNA. To analyze the correlation functions in this case the diffusion coefficient  $\tau_2$  of the complex was calculated from the diffusion coefficient  $\tau_1$  of the DNA and the ratio  $\tau_2/\tau_1 = 1.46 \pm 0.11$ . This ratio was determined from FCS measurements where both the free DNA and the fully protein-saturated DNA were measured, so that the data could be fitted to a one component model (equation 6,  $\theta = 0$  or  $\theta = 1$ ). The average  $K_d$  of  $7.3 \pm 2.5$  nM determined by FCS at 600 mM K acetate is in good agreement with the corresponding value of  $4.2 \pm 0.9$  nM from the FA measurements. The dissociation constants of wt-NtrC to the ES-1<sub>rho</sub> DNA duplex with a single binding site derived from both FA and FCS measurements are summarized in Table 1. The data demonstrate that  $K_d$  decreases with increasing salt concentration.

**Table 1.** Dissociation constants for binding of wild-type NtrC to ES-1<sub>rho</sub><sup>a</sup>

Potassium acetate concentration (mM)	Dissociation constant $K_d$ (nM)
15	$0.014 \pm 0.010$
50	0.21 <sup>b</sup>
150	$0.46 \pm 0.32$
600	$5.8 \pm 2.6$

<sup>a</sup>Average values from FA and FCS measurements at 25°C in a solution containing 10 mM Tris-acetate, pH 8.0, 0.1 mg/ml BSA, 1 mM DTT, 0.1 mM EDTA and 0.1% NP-40.

<sup>b</sup>Measured in 50 mM Tris-HCl, pH 8.0, 50 mM KCl, 5 mM MgCl<sub>2</sub>, 0.1 mM EDTA and 2 mM ATP at 20°C (18).

A theoretical treatment for the dependence of binding affinity from the monovalent ion concentration has been derived by Record and co-workers (47,48).

$$\partial \log K_d / \partial \log [M^+] = z\psi \quad 9$$

According to this equation a double logarithmic plot of the binding constant  $K_d$  versus the salt concentration  $[M^+]$  is linear. The slope of this plot yields the number of ion pairs  $z$  that are formed upon binding. The double logarithmic plot of the data from Table 1 is shown in Figure 4. Previously the dissociation constant for this binding site has been measured by a nitrocellulose filter binding assay (18) at 50 mM monovalent ion concentration. This value has also been included in the plot. Using 0.88 for the parameter  $\psi$  for double-stranded B-form DNA (47) we obtained a value of 1.8 for  $z$  by linear regression analysis. Thus two ion pairs are formed upon binding of the protein to the DNA.

### Binding of NtrC to two adjacent binding sites

For these studies DNA fragment ES-2<sub>rho</sub> was used, which carries two adjacent binding sites (site Lp) with a center to center distance of 32 bp. Figure 5 shows the titration curves monitored by FA for wild-type and mutant protein under the same reaction conditions as those used for the study of stoichiometric binding to one DNA binding site presented in Figure 2A, namely at a DNA concentration of 10 nM ES-2<sub>rho</sub> duplex and in the presence of 150 mM potassium acetate.

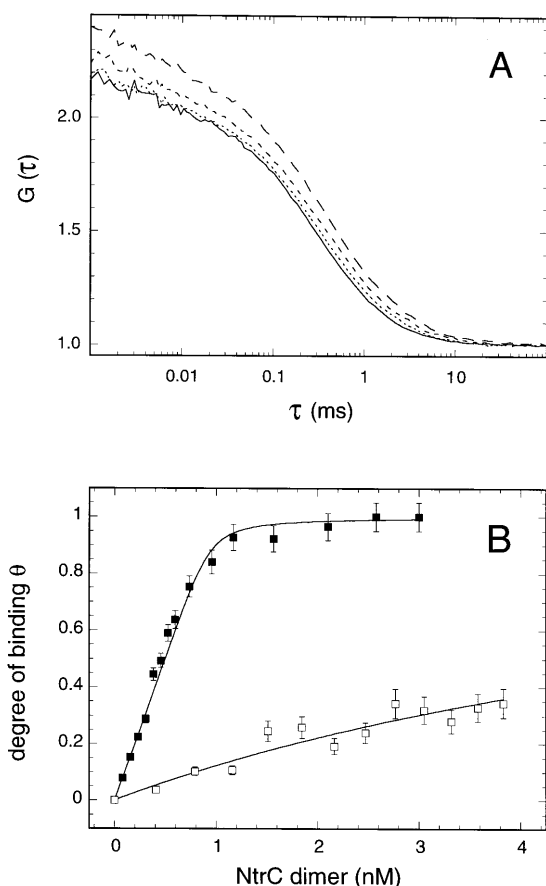


**Figure 3.** Fluorescence correlation spectroscopy of wild-type NtrC-DNA complexes. Measurements were made with a 1 nM ES-1<sub>rho</sub> solution. (A) Correlation functions. The percentage of DNA complexed with NtrC protein was determined by a two component fit to each function. Curves for 0 (—), 40 (.....), 80 (---) and 100% (- - -) wt-NtrC-ES-1<sub>rho</sub> complex are shown. (B) Titration curves derived from the correlation functions. The solution contained the standard buffer supplemented with 15 mM (■) or 600 mM (□) potassium acetate. The curve shows the fit according to the expected degree of binding for a single site (equation 8). Mean values of  $0.014 \pm 0.01$  nM (15 mM K acetate) and  $7.3 \pm 2.5$  nM (600 mM K acetate) were determined for the dissociation constant  $K_d$ .

Analysis of the data revealed that binding to the two adjacent binding sites in ES-2<sub>rho</sub> was more complex due to formation of multiple species. The binding curve for wild-type NtrC (Fig. 5) displayed a characteristic shape. During addition of one equivalent of protein (10 nM dimer) to the 10 nM ES-2<sub>rho</sub> duplex (= 20 nM binding sites) a steep linear increase in anisotropy was observed with a relatively high anisotropy value at 10 nM added NtrC dimer. At this protein concentration and under conditions of stoichiometric binding the concentration of complexes where only one NtrC dimer was bound per DNA duplex should reach its maximum. The ratio of this species to complexes that have two dimers bound depends on the cooperativity of binding. Upon addition of the second equivalent of protein to a concentration of 20 nM almost all binding sites were saturated and DNA complexes were formed that have two NtrC dimers. This process was accompanied by only a small increase in fluorescence anisotropy. Two important conclusions can be made to explain the

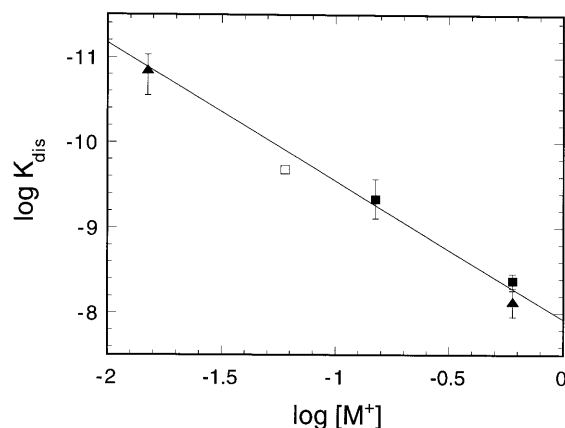


**Figure 4.** Dependence of the binding constant of wild-type NtrC on the ion concentration. Data were taken from Table 1. The FA data are represented by (■), the value measured by Weiss *et al.* (18) is indicated by (□) and (▲) shows data measured by FCS.

strong increase in anisotropy from 0 to 10 nM protein: the cooperativity of the binding process was low and anisotropy of the species with a single NtrC dimer was only slightly smaller than that of the corresponding complex with two dimers. After addition of 20 nM NtrC dimer a plateau value was reached and further addition of proteins led to only a minimal increase in anisotropy. This indicates that only two dimers could bind to the DNA. For a more quantitative analysis of the binding curves a two step binding model was fitted to the data as described in Materials and Methods. The microscopic binding constant for the single site determined from the experiments with DNA fragment ES-1<sub>rho</sub> was used, i.e. the macroscopic binding constant  $K_1$  for the first step (equation 4) was set to 0.23 nM. For the second step values of  $K_2 \sim 10^{-9}$  M were obtained from the fit, corresponding to a cooperativity constant  $k_{12}$  of the order of 0.3–1.5 as defined in equation 4. Thus according to the titrations presented here we observed no cooperativity for binding of wild-type NtrC. We obtained an anisotropy of 0.196–0.197 for the complex of ES-2<sub>rho</sub> with one NtrC dimer from the fit. The corresponding anisotropy of the complex containing two dimers was only slightly larger, at  $\sim 0.203$ . This result is in agreement with the much smaller relative change of volume from the complex with one protein dimer bound to that with two bound dimers. From these values and the form of the binding isotherm we conclude that during addition of the first equivalent of protein primarily the dimeric complex was present. Addition of the second equivalent of protein then led to formation of the final complex where both binding sites were occupied.

Mutant NtrC<sup>S160F</sup> showed a rather different binding isotherm (note also the difference in the scale of the x-axis between Fig. 5A and B). Up to addition of two equivalents of protein (20 nM) the anisotropy increased linearly. This increase in anisotropy then became smaller, but did not reach a plateau even after a 6-fold excess of protein had been added. In the experiments with a single binding site duplex (see above) it was shown that the binding constant for binding of one dimer to a single site was the same for wt-NtrC and the NtrC<sup>S160F</sup> mutant. Accordingly, the linear part at the start of the titration of ES-2<sub>rho</sub> duplex in Figure 5B has to be assigned to quantitative formation of a complex containing two NtrC<sup>S160F</sup> dimers and one DNA fragment. This implies a high

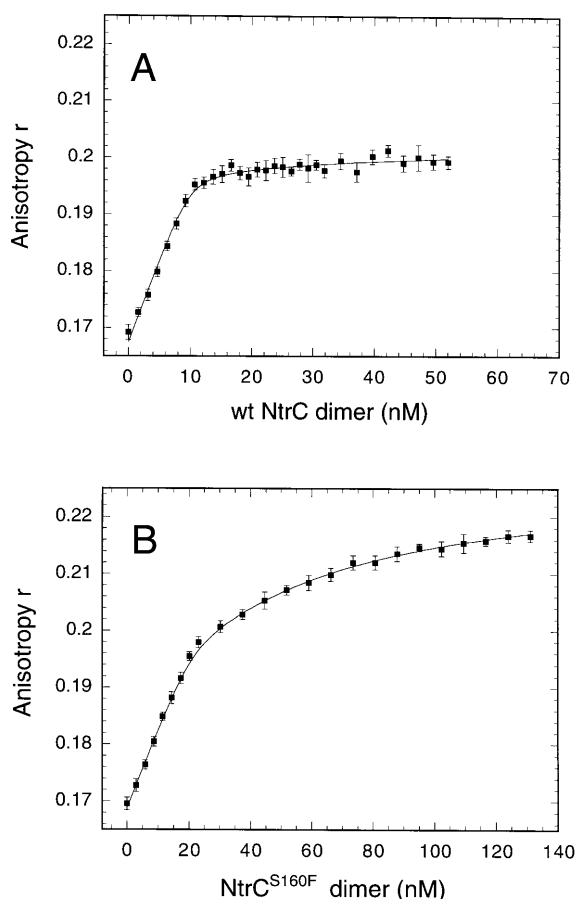


**Figure 5.** Anisotropy curves for binding of NtrC to the enhancer site ES-2<sub>rho</sub>. The solutions contained 150 mM potassium acetate and 10 nM ES-2<sub>rho</sub> duplex. The solid curves correspond to a fit of the data with the program BIOEQS according to the model described in the text. (A) Titration with wild-type NtrC. The macroscopic dissociation constant  $K_1$  for binding of the first dimer (see equations 2 and 4) was fixed at  $2.3 \times 10^{-10}$  M, the value determined from titrations with duplex ES-1<sub>rho</sub>. (B) Titration with NtrC<sup>S160F</sup>.

positive cooperativity for binding of the second protein to the DNA ( $k_{12} > 40$ ), because here the intermediate species with one bound protein was not observed. After addition of two equivalents of dimer anisotropy increased further, indicating that more proteins were binding to the complex containing two bound dimers. The stoichiometry of this higher order oligomeric complex could not be resolved unequivocally from the binding isotherm, but the data were consistent with formation of a tetramer of dimers according to equation 5, as was assumed in the fit shown in Figure 5B. For this model the value of  $K_3$  (equation 5) was  $\sim 2 \times 10^{-8}$  M<sup>2</sup>.

#### Anisotropy values of the different species

Comparing the absolute anisotropy values of the species investigated, it was apparent that anisotropy of the short oligonucleotide duplex ES-1<sub>rho</sub> ( $r = 0.18$ ) was higher than that of the longer oligonucleotide duplex ES-2<sub>rho</sub> ( $r = 0.17$ ), although ES-1<sub>rho</sub> is shorter than ES-2<sub>rho</sub> (32 versus 59 bp). In addition, the complex of ES-1<sub>rho</sub> with one NtrC dimer had a higher FA than the larger complex of ES-2<sub>rho</sub> with two protein dimers bound ( $r = 0.21$  versus 0.20). The high anisotropies found generally for rhodamine-

labeled oligonucleotide duplexes indicate a relatively strong interaction of the dye with the DNA, as has been observed in other studies of rhodamine dyes covalently linked to DNA (see for example 49). With the C<sub>6</sub> aminoalkyl linker used here an interaction with approximately the first 5 bp next to the label is geometrically possible. This interaction might cause a change in the rotational freedom of the dye as well as a modified lifetime. Bigger rotational freedom or longer lifetimes would result in smaller values of anisotropy for this species. Since the sequence next to the label is different for the two duplexes (ES-1<sub>rho</sub>, rho-TGAGA; ES-2<sub>rho</sub>, rho-TCAGT), this may explain the observed absolute values of  $r$ . For interpretation of the titration curves the differences in absolute anisotropy values are not relevant, since for the analysis it is only required that the  $r$  values are significantly different for the species presented in one mixture at equilibrium.

#### DISCUSSION

The application of FA and FCS measurements to analyzing binding of NtrC to its enhancer site yields quantitative information about the system free in solution and at thermodynamic equilibrium. No modification of the protein is required and the fluorescently labeled DNA duplexes are readily available from commercial sources. The techniques are non-invasive and salt concentration, pH and temperature can be varied over a wide range. This has been demonstrated here by measuring binding constants under high salt conditions with two different DNA oligonucleotide duplexes and by detection of protein–DNA complexes containing higher order oligomers of NtrC<sup>S160F</sup> in solution.

The concentration of active NtrC dimers was determined by stoichiometric titration with single binding site ES-1<sub>rho</sub> (Fig. 2A). This method showed high reproducibility with various protein preparations. Single binding site ES-1<sub>rho</sub> was used to compare binding affinity to DNA of wild-type NtrC and the constitutive mutant NtrC<sup>S160F</sup>. At 600 mM salt concentration we found no difference in affinity for the single binding site. This confirms previous studies that have shown identical strength of binding for wild-type NtrC and the transcriptionally active phosphorylated form of NtrC (18). These studies were conducted under much lower salt conditions (50 mM KCl) and we conclude that affinity of binding changes identically for both wild-type and mutant forms of the protein upon change of the ion concentration. This result is consistent with the idea that DNA binding of NtrC is mediated by a distinct C-terminal protein domain homologous to that of FIS. The S160F mutation in the activation domain is not expected to have an effect on DNA binding to a single site (4).

A number of studies have been published utilizing FA to study binding (24,25,50) and oligomerization (26) of a protein to DNA, whereas FCS to our knowledge has not been used previously to quantitate protein–DNA interactions. In the work reported here we have demonstrated how FCS curves can be evaluated to determine dissociation constants for protein–DNA interactions. The dissociation constants obtained by FA and FCS for binding of wt-NtrC to a single DNA site are the same within experimental error. Thus FCS is a suitable method to study this type of system. The errors in estimating the degree of binding were about twice as high as for FA measurements. This is mostly due to the fact that the difference in diffusion time between free DNA and the protein–DNA complex is small. The fairly large standard deviation in the FCS measurements conducted at 15 mM salt also

reflects the fact that titration curves do not vary to a large degree when the DNA concentration exceeds the dissociation constant  $K_d$ . Furthermore, the DNA concentration has to be known precisely, since it enters the fitting function (equation 1 or 8).

In this respect it would be advantageous to conduct the experiments under conditions where the DNA concentration could be neglected, i.e. under conditions where the concentration of free protein  $P_{\text{free}}$  is approximately equal to the total protein concentration. This is the case if the total DNA concentration  $D_{\text{tot}}$  is at least 10 times lower than the  $K_d$ . For binding of NtrC this would require a DNA concentration of  $10^{-11}$ – $10^{-12}$  M, since the  $K_d$  is of the order of  $10^{-10}$ – $10^{-11}$  M under physiological salt concentrations (Table 1). With our experimental set-up the fluorescence signal at picomolar DNA concentrations was too low and we found that the limit was around 1 nM (FA) and 0.1 nM (FCS) rhodamine-labeled DNA for reliable measurements. Using laser excitation instead of a xenon lamp for the FA measurements it is possible to reduce the DNA concentration by about a factor of 10 to ~0.1 nM (50). However, this is still in the range where the DNA concentration has to be accurately known for analysis, which can be difficult for DNA concentrations <1 nM due to non-specific binding of the DNA to the cuvettes or cover slides. As deduced from FCS measurements (51), the error is significant for dye concentrations <0.1 nM, even if non-specific binding of the DNA (and the protein) is suppressed by addition of BSA and/or detergents or by silylation of the cuvettes, as was done for the experiments described here. Thus the DNA concentrations used here in the range 1–10 nM are a compromise to yield a good signal-to-noise ratio and to avoid a reduction in the DNA concentration due to non-specific binding. In principle the FCS technique can be used for measurements at picomolar dye concentrations and below with very small sample volumes (50–100  $\mu$ l). Thus FCS appears to be ideally suited to the analysis of high affinity protein–DNA interactions and we are currently exploring the possibility of this exciting technique with an improved instrument (51).

The two fluorescence techniques described here for analysis of NtrC–DNA binding are true equilibrium methods that work over a large range of solution conditions. In particular, the salt concentration can be varied over a large concentration range. We found that the logarithm of the dissociation constant  $K_d$  for binding of wt-NtrC to a single site depended linearly on the logarithm of the salt concentration, as shown for other protein–DNA interactions (47,48). Our results indicate that one dimer of NtrC forms two ion pairs with the DNA backbone upon binding. Assuming a similar folding for FIS and the C-terminal DNA binding domain of NtrC one can predict that NtrC, like FIS, carries a stretch of basic amino acids on the surface contacting the DNA. Two of these basic residues in NtrC, K445 and K464, correspond to residues Q74 and K93 in FIS, predicted to contact the DNA backbone (4,52) [note that the *Escherichia coli* NtrC sequence given in North *et al.* (4) has been revised (53)]. Thus these residues are likely candidates for the two ion pairs (one per NtrC monomer) which form upon binding of NtrC to DNA, as deduced from the salt dependence of the dissociation constants.

Anisotropy curves for unphosphorylated wild-type NtrC confirm that one dimer binds to one DNA binding site and two dimers to two adjacent binding sites (16,17). Previously it was reported that binding of two unphosphorylated NtrC dimers to the enhancer is cooperative, with a cooperativity constant of 20–100 as determined by gel shift experiments, nitrocellulose filter binding assays and

quantitative DNA footprinting (17–19). In contrast to these results, we found that binding of NtrC to the ES-2<sub>rho</sub> duplex occurred essentially without cooperativity ( $k_{12} = 0.3$ – $1.5$ ). For comparison of the data one important parameter is the presence of ATP in the binding buffer. The studies cited above report a cooperativity constant of 20 (17), 37 (18) and 100 (19) in the presence of 2 mM ATP. In the absence of ATP the cooperativity constant decreased from 100 to 20 (19). The values obtained by Weiss *et al.* (18) and Chen and Reitzer (19) were determined for a somewhat different sequence of NtrC binding sites as compared with the ES-2<sub>rho</sub> duplex studied here. The sequence of ES-2 is identical to the 106 bp DNA fragment analyzed in Porter *et al.* (17) but is lacking part of the DNA region flanking the NtrC binding sites. Since a cooperativity constant of 20 has been determined for this sequence by gel shift experiments in the presence of ATP (17), it appears reasonable to assume that the corresponding value in the absence of ATP would be significantly lower and in the range of the values determined here. In addition, it should be considered that the methods used previously for analysis of DNA binding of NtrC are not true equilibrium methods, in contrast to FA and FCS measurements.

Anisotropy curves for the NtrC<sup>S160F</sup> mutant display a high cooperativity of binding and reveal formation of oligomers on the single DNA binding site and on the two adjacent binding sites in the ES-2<sub>rho</sub> duplex. The cooperativity factors for the phosphorylated protein have been reported (17,18), but differ by several orders of magnitude. For the S160F mutant cooperativity was found to be 52 (17). This value is in agreement with our measurements for the transcriptionally active NtrC<sup>S160F</sup> mutant, for which a value of  $k_{12} > 40$  has been estimated.

The results of the FA measurements with mutant NtrC<sup>S160F</sup> are consistent with formation of an octameric complex, which has been suggested for phosphorylated NtrC on the basis of electron microscopic analysis (6), scanning force microscopy (21) and analytical ultracentrifugation (16). However, the FA data did not allow an accurate determination of the molecular weight of the complex formed by NtrC<sup>S160F</sup> on the enhancer sequence ES-2<sub>rho</sub>. The importance of protein–protein interactions for the biological activity of NtrC has been demonstrated previously by showing synergistic activation of a mixture of a weakly transcriptionally active mutant and a non-DNA binding mutant (17,21). From our measurements on the NtrC<sup>S160F</sup> mutant we estimate that the concentration of NtrC dimers has to be  $>10^{-8}$  M for quantitative formation of the octameric complex. This would be significantly weaker than binding of two dimers to the enhancer site, which occurs in the sub-nanomolar region. Assuming a volume of  $1 \mu\text{m}^3$  for a single *E. coli* cell, the intracellular concentration of NtrC can be calculated to be 10 nM in the inactive state (15). Under nitrogen limiting conditions it rises to 100 nM. Thus it appears possible that this concentration increase is part of the regulatory mechanism. However, as discussed above, our results have been obtained in the absence of ATP, which is present in the bacterial cell at a concentration of ~2 mM. Since it has been shown with NtrC<sup>S160F</sup> from *Klebsiella pneumoniae* that ATP $\gamma$ S is able to promote formation of higher order oligomers (54), the effect of ATP on the DNA binding properties of NtrC is an important parameter that remains to be studied in further detail. In addition, we conclude from analytical ultracentrifugation experiments (16) that the phosphorylated wild-type protein forms an octameric complex on the enhancer with high cooperativity and in the absence of ATP. Thus it appears likely that the association

properties of the NtrC<sup>S160F</sup> mutant and the phosphorylated wild-type protein are rather different.

## ACKNOWLEDGEMENTS

We are grateful to Catherine Royer for providing the BIOEQS program and for her help in using it, Sydney Kustu and Anne North for a plasmid clone with the NtrC<sup>S160F</sup> gene and Alexandra Schulz and Katalin Tóth for critical reading of the manuscript. We also thank the companies Zeiss and Evotec for providing the FCS Confocor instrument used in this study. This work was supported by a fellowship from the Cusanuswerk to F.W.S.

## REFERENCES

- Magasanik, B. (1996) In Neidhardt, F.C. (ed.), *Escherichia coli and Salmonella*. ASM Press, Washington, DC, Vol. 1, pp. 1344–1356.
- Wedel, A., Weiss, D.S., Popham, D., Dröge, P. and Kustu, S. (1990) *Science*, **248**, 486–490.
- Reitzer, L.J. and Magasanik, B. (1986) *Cell*, **45**, 785–792.
- North, A.K., Klose, K.E., Stedman, K.M. and Kustu, S. (1993) *J. Bacteriol.*, **175**, 4267–4273.
- Collado-Vides, J., Magasanik, B. and Gralla, J.D. (1991) *Microbiol. Rev.*, **55**, 371–394.
- Su, W., Porter, S., Kustu, S. and Echols, H. (1990) *Proc. Natl. Acad. Sci. USA*, **87**, 5504–5508.
- Rippe, K., Guthold, M., von Hippel, P.H. and Bustamante, C. (1997) *J. Mol. Biol.*, **270**, 125–138.
- Ninfa, A.J. and Magasanik, B. (1986) *Proc. Natl. Acad. Sci. USA*, **83**, 5909–5913.
- Sanders, D.A., Gillice, C.B., Burlingame, A.L. and Koshland, D.J. (1992) *J. Bacteriol.*, **174**, 5117–5122.
- Weiss, V. and Magasanik, B. (1988) *Proc. Natl. Acad. Sci. USA*, **85**, 8919–8923.
- Keener, J. and Kustu, S. (1988) *Proc. Natl. Acad. Sci. USA*, **85**, 4976–4980.
- Weglanski, P., Ninfa, A.J., Ueno, N.S. and Magasanik, B. (1989) *J. Bacteriol.*, **171**, 4479–4485.
- Klose, K.E., Weiss, D.S. and Kustu, S. (1993) *J. Mol. Biol.*, **232**, 67–78.
- Moore, J.B., Shiao, S.P. and Reitzer, L.J. (1993) *J. Bacteriol.*, **175**, 2692–2701.
- Reitzer, L.J. and Magasanik, B. (1983) *Proc. Natl. Acad. Sci. USA*, **80**, 5554–5558.
- Rippe, K., Mücke, N. and Schulz, A. (1998) *J. Mol. Biol.*, submitted for publication.
- Porter, S.C., North, A.K., Wedel, A.B. and Kustu, S. (1993) *Genes Dev.*, **7**, 2258–2273.
- Weiss, V., Claverie-Martin, F. and Magasanik, B. (1992) *Proc. Natl. Acad. Sci. USA*, **89**, 5088–5092.
- Chen, P. and Reitzer, L.J. (1995) *J. Bacteriol.*, **177**, 2490–2496.
- Mettke, I., Fiedler, U. and Weiss, V. (1995) *J. Bacteriol.*, **177**, 5056–5061.
- Wyman, C., Rombel, I., North, A.K., Bustamante, C. and Kustu, S. (1997) *Science*, **275**, 1658–1661.
- Révet, B., Brahms, S. and Brahms, G. (1995) *Proc. Natl. Acad. Sci. USA*, **92**, 7535–7539.
- Perrin, F. (1926) *J. Phys. Radiat.*, **1**, 390–401.
- Heyduk, T. and Lee, J.C. (1990) *Proc. Natl. Acad. Sci. USA*, **87**, 1744–1748.
- Heyduk, T., Lee, J.C., Ebricht, Y.W., Blatter, E.E., Zhou, Y. and Ebricht, R.H. (1993) *Nature*, **364**, 548–549.
- LeTilly, V. and Royer, C.A. (1993) *Biochemistry*, **32**, 7753–8.
- Benight, A.S., Langowski, J., Wu, P.G., Wilcoxon, J., Shibata, J.H., Fujimoto, N.S., Ribeiro, N.S. and Schurr, J.M. (1987) In Stepanek, J., Anzenbacher, P. and Sedlacek, B. (eds), *Laser Scattering Spectroscopy of Biological Objects*. Elsevier, Amsterdam, The Netherlands, Vol. 45, pp. 407–422.
- Aragon, S.R. and Pecora, R. (1976) *J. Chem. Phys.*, **64**, 1791–1803.
- Elson, E.L. and Magde, D. (1974) *Biopolymers*, **13**, 1–27.
- Ehrenberg, M. and Rigler, R. (1974) *Chem. Phys.*, **4**, 390–401.
- Rigler, R., Widengren, J. and Mets, Ü. (1992) In Wolfbeis, O.S. (ed.), *Fluorescence Spectroscopy*. Springer, Berlin, Germany.
- Rigler, R. and Widengren, J. (1990) *BioScience*, **3**, 180–183.
- Kinjo, M. and Rigler, R. (1995) *Nucleic Acid Res.*, **23**, 1795–1799.
- Klingler, J. and Friedrich, T. (1997) *Biophys. J.*, **73**, 2195–2200.
- Maiti, S., Haupts, U. and Webb, W.W. (1997) *Proc. Natl. Acad. Sci. USA*, **94**, 11753–11757.
- Sterrer, S. and Henco, K. (1997) *J. Recept. Signal Transduct. Res.*, **17**, 511–520.
- Eigen, M. and Rigler, R. (1994) *Proc. Natl. Acad. Sci. USA*, **91**, 5740–5747.
- Rentzeperis, D., Rippe, K., Jovin, T.M. and Marky, L.A. (1992) *J. Am. Chem. Soc.*, **114**, 5926–5928.
- Puglisi, J.D. and Tinoco, L., Jr (1989) *Methods Enzymol.*, **180**, 304–325.
- Rippe, K., Ramsing, N.B. and Jovin, T.M. (1989) *Biochemistry*, **28**, 9536–9541.
- Flashner, Y., Weiss, D.S., Keener, J. and Kustu, S. (1995) *J. Mol. Biol.*, **249**, 700–713.
- Gill, S.C. and von Hippel, P.H. (1989) *Anal. Biochem.*, **182**, 319–326.
- Ackers, G.K., Shea, M.A. and Smith, F.R. (1983) *J. Mol. Biol.*, **170**, 223–242.
- Royer, C.A. and Beechem, J.M. (1992) *Methods Enzymol.*, **210**, 481–505.
- Royer, C.A. (1993) *Anal. Biochem.*, **210**, 91–97.
- Widengren, J., Mets, Ü. and Rigler, R. (1995) *J. Phys. Chem.*, **99**, 13368–13379.
- Record, M.T.J., Lohman, M.L. and De Haseth, P. (1976) *J. Mol. Biol.*, **107**, 145–158.
- Lohman, T.M. and Mascotti, D.P. (1992) *Methods Enzymol.*, **212**, 400–425.
- Vámosi, G., Gohlke, C. and Clegg, R.M. (1996) *Biophys. J.*, **71**, 972–994.
- Reedstrom, R.J., Brown, M.P., Grillo, A., Roen, D. and Royer, C.A. (1997) *J. Mol. Biol.*, **273**, 572–585.
- Tewes, M. (1997) PhD thesis, University of Heidelberg, Heidelberg, Germany.
- Pan, C.Q., Finkel, S.E., Cramton, S.E., Feng, J.A., Sigman, D. and Johnson, R.C. (1996) *J. Mol. Biol.*, **264**, 675–695.
- Blattner, F.R., Plunkett, G.R., Bloch, C.A., Perna, N.T., Burland, V., Riley, M., Collado-Vides, J., Glasner, J.D., Rode, C.K., Mayhew, G.F., Gregor, J., Davis, N.W., Kirkpatrick, H.A., Goeden, M.A., Rose, D.J., Mau, B. and Shao, Y. (1997) *Science*, **277**, 1453–1474.
- Farez-Vidal, M.E., Wilson, T.J., Davidson, B.E., Howlett, G.J., Austin, S. and Dixon, R.A. (1996) *Mol. Microbiol.*, **22**, 779–788.